CU Journal of Non-Linear Fluid Mechanics
Vol. 01, No. 02, 2025
https://doi.org/10.11615/cujnlfm.01203-6

Heat Transfer Augmentation in Forced Convection Flow Using a Dilute Aqueous Suspension of Molybdenum Disulphide Nanoparticles

Neha Elizabeth Sam[a] and Roxanne Francis *[b]

[a] Centre for Mathematical Needs, Department of Mathematics, Christ University, Hosur Road, Bengaluru, Karnataka 560029, India.
[b] Department of Mathematics, The University of the West Indies, Mona Campus, Kingston 7, St. Andrew, State, Kingston, Jamaica

Abstract

This paper presents a numerical investigation of forced convection heat transfer in a water-based molybdenum disulphide (MoS_2) nanofluid flowing through a three-dimensional porous enclosure. The flow is governed by the non-Darcy regime, modeled using the Darcy-Brinkman-Forchheimer (DBF) equation, while the energy equation is formulated under the local thermal equilibrium assumption. The highly nonlinear coupled system of equations is solved using a finite difference method (FDM) with a uniform grid, enhanced by the Alternating Direction Implicit (ADI) scheme for computational efficiency. A systematic grid independence study is conducted to ensure solution accuracy. The results quantify the enhancement of thermal performance, demonstrating that the Nusselt number increases significantly with higher nanoparticle volume fractions, greater geometric complexity of the porous medium (shape factor), and increased inertial effects (Forchheimer number). The study conclusively establishes that the use of water-MoS_2 nanofluids in structured porous media is a highly effective strategy for augmenting heat transfer, with promising applications in the design of advanced thermal management systems.

Keywords: Darcy-Brinkman-Forchheimer Model; Water-MoS_2 Nanofluid; Porous Media Heat Transfer; Finite Difference Method; Nusselt Number

1 Introduction

Modern energy systems, such as the Rankine cycles in thermal power plants and the cooling of photovoltaic panels and power inverters, all depend on being able to efficiently capture and reject heat. Liquid coolants are common in these roles, but their effectiveness is limited by a basic property of the material: thermal conductivity. To address this limitation, the traditional approach of using pure liquids is being replaced by the progress of functionalised fluid composites. One of the most important new ideas in this field is to mix ultrafine solid particles between 1 and 100 nanometers in size to make a new type of heat transfer fluid that works much better. The choice of nanoparticles as additives is mainly due to their much higher thermal conductivity compared to base fluids, as shown in earlier research [1], [2],[3]. These nanoparticle suspensions, known as "nanofluids" (a term introduced by Choi and Eastman [4]), represent an innovative

* roxanne.francis@uwimona.edu.jm

category of engineered coolants. Research into nanofluids has grown a lot in the last few years because they can be used in many different fields, including medicine and industry. Due to this, they are widely thought to be new working fluids that can improve thermal performance in many thermal and flow systems. Nanoliquids are considered potential and innovative fluids that improve thermal performance in applications where efficient heat transfer is important, such as heating and cooling systems with heat exchangers and solar energy devices [5]. The existing literature indicates that theoretical and numerical investigations of heat transfer in nanoliquids predominantly rely on three principal modeling methodologies: the single-phase model introduced by Khanafer, Vafai, and Lightstone [6][7]; the two-phase Buongiorno model[8]; subsequent adaptations of the Buongiorno framework [9] and also recent studies extended to the investigation of chaos in convection using nanoliquids [10].

The transport of fluids within porous structures is a subject that has been studied for quite some time. The Brinkman– Forchheimer equation has become one of the most important models for understanding this type of phenomenon. The Darcy law was first introduced by Darcy [11] in the 19th century, but it was later extended to include other physical effects, such as boundary interactions, viscous diffusion, and inertial contributions [12][13]. Further studies conducted by Vafai and Tien [14] and Rudraiah et al. [15] improved the theoretical understanding of porous medium flows by including the solid boundary and inertia effects inside the porous matrix. Their work used local volume-averaging techniques to derive the governing equations near impermeable surfaces, discussing important physical assumptions and limitations of the model. Despite these advancements in theory and experiments, solving the Brinkman–Forchheimer equation itself is still a great challenge because of its nonlinearity property, especially for two- and three-dimensional geometries (Bear and Bachmat [16]). These computational difficulties have motivated strong numerical methods development. Among them, central difference approximation has been popularly used to discretize the governing partial differential equations of fluid motion (Patankar [17]). On another front, finite element method applications to problems concerning porous media are very numerous since this method allows high spatial accuracy when dealing with irregular geometries. Another evolution related to numerical modeling is quasi-linearization techniques introduced by Bellman and Kalaba [18]. Nonlinear governing equations can be converted into a series of linear subproblems under this approach so that efficient iterative computations can be performed when combined with finite difference or finite element schemes; therefore such formulations will present practical ways toward finding converging solutions which are stable computationally applicable on complex flow systems governed under Darcy–Forchheimer–Brinkman frameworks. Sam et al. [19] have recently expanded these numerical methods to more complex geometries. These studies highlight the flexibility and increasing significance of modified finite difference and quasi-linearization techniques in forecasting flow and heat transfer behavior in porous media systems that hold practical engineering importance.

The current paper employs the FDM. As with the FEM, the FDM may also be used ineffectively manage the geometry and boundary conditions. This method can be coupled with the Alternate Direct Implicit (ADI) method, which provides stability and efficiency when solving large systems iteratively (see Jain et al. [20]). The modified

FDM that uses a quasi-linearization procedure can model flow equations more accurately in a rectangular enclosure, thus increasing solution accuracy significantly in geometrically complex domains. This study extends previous work on Brinkman–Forchheimer flows of Newtonian fluids through an enclosure by introducing two straight boundaries and one curved boundary. An application of modified FDM here is intended to enhance understanding of the Brinkman-Forchheimer flow dynamics and assist in developing accurate and efficient numerical models for fluid flow through porous media The present study attempts to address existing research gaps regarding Brinkman-Forchheimer flows within rectangular enclosures possessing both straight surfaces. The following points encapsulate the novelty and importance of this work. Explores Brinkman–Forchheimer flow of a water–MoS_2 nanofluid inside a rectangular porous enclosure. Uses the finite difference method with ADI scheme, achieving high accuracy (10^{-4}). Reports that Nusselt number increases with nanoparticle volume fraction, shape factor and Forchheimer number; explains effects of porous resistance and inertial effects on flow and heat transfer behaviour.

2 Nomenclature

Symbol	Description (SI Units)	Symbol	Description (SI Units)
(x,y,z)	Cartesian coordinates (m)	T	Temperature (K)
h,k	Step length (m)	T_w	Wall temperature (K)
p	Pressure (Pa)	T_m	Mean temperature (K)
w	Velocity component (m/s)	Pe	Peclet number (dimensionless)
(X,Y,Z)	Scaled coordinates (dimensionless)	θ	Dimensionless temperature (dimensionless)
μ_{nf}	Nanofluid dynamic viscosity (Pa·s)	Nu	Nusselt number (dimensionless)
C_b	Ergun drag coefficient (dimensionless)	q	Heat flux (W/m^2)
K	Permeability of porous medium (m^2)	k_{nf}	Nanofluid thermal conductivity (W/m·K)
u_R	Reference velocity (m/s)	Y	Aspect ratio (dimensionless)
Λ	Brinkman number (dimensionless)	n	Number (dimensionless)
σ^2	Porous parameter (dimensionless)	m	Mean (varies)
Re	Reynolds number (dimensionless)	w	Wall (subscript)
F	Forchheimer number (dimensionless)		
s	Shape factor (dimensionless)		
Ω	Cross-sectional area (m^2)		

3 Mathematical formulation

This study examines the steady, fully developed flow of a nanofluid within a three-dimensional porous rectangular enclosure. The domain, illustrated in Figure 1, has finite dimensions $a \times b$ in the (x,y)-plane and is infinitely extended along the z-axis. Define

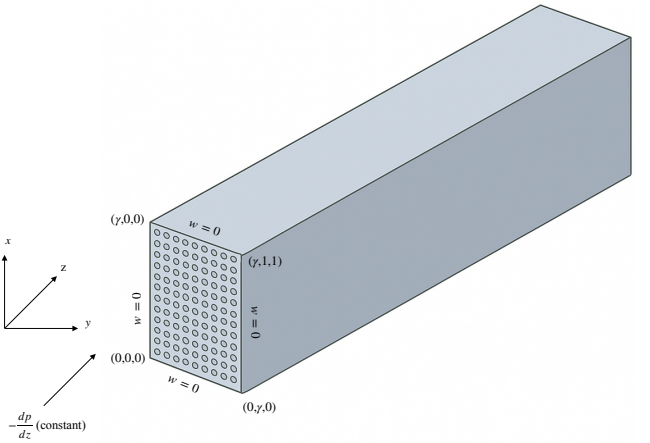

Figure 1: Problem setup: geometry and boundary conditions for flow in a porous medium.

$R = \{(x,y,z) \,|\, 0 \le x \le a,\ 0 \le y \le b,\ 0 \le z < \infty\}$, the enclosure features impermeable walls at $x = 0$, $x = a$, $y = 0$, and $y = b$. The momentum transport in the z-direction is governed by the Darcy-Brinkman-Forchheimer (DBF) equation.

$$\mu'_{nf}\left(\frac{\partial^2 w}{\partial x^2} + \frac{\partial w^2}{\partial y^2}\right) - \frac{\mu_{nf}}{K_{nf}}w - \frac{\rho_{nf}C_b}{\sqrt{K_{nf}}}w^2 = \frac{dp}{dz}. \tag{1}$$

The governing equations are normalized using the following dimensionless variables:

$$X = \frac{x}{a}, \quad Y = \frac{y}{b}, \quad W = \frac{w}{u_R}, \quad P = \frac{pa}{\mu_{nf}u_R}. \tag{2}$$

Substituting these dimensionless variables into Eq. (1) yields the non-dimensional momentum equation:

$$\frac{\partial^2 W}{\partial X^2} + \gamma^2\frac{\partial^2 W}{\partial Y^2} - \Lambda_{nf}\sigma^2_{nf}W - C_b Re\sigma_{nf}W^2 = -P^*, \tag{3}$$

where $P^* = -\frac{\partial p}{\partial z}$ is the dimensionless pressure gradient. The governing parameters in the equation are defined as follows:

$$\gamma = \frac{a}{b} \qquad \text{(Aspect ratio)}, \tag{4}$$

$$\Lambda = \frac{\mu_{nf}}{\mu'_{nf}} \qquad \text{(Viscosity ratio)}, \tag{5}$$

$$\sigma^2_{nf} = \frac{a^2}{K_{nf}} \qquad \text{(Inverse Darcy number)}, \tag{6}$$

$$Re = \frac{\rho u_R a}{\mu'_{nf}} \qquad \text{(Reynolds number)}, \tag{7}$$

with C_b representing the Forchheimer drag coefficient.

Substituting the scaled velocity $\widetilde{W} = W/P^*$ into Eq. (17) results in:

$$\frac{\partial^2 \widetilde{W}}{\partial X^2} + \gamma^2 \frac{\partial^2 \widetilde{W}}{\partial Y^2} - s_{nf}^2 \widetilde{W} - F s_{nf} \widetilde{W}^2 = -\Lambda_{nf}, \tag{8}$$

where the key dimensionless parameters are:

$$F = C_b Re \frac{\sigma}{\sqrt{\Lambda_{nf}}} P^* \qquad \text{(Forchheimer number)}, \tag{9}$$

$$s_{nf} = \sqrt{\Lambda_{nf}} \sigma_{nf} \qquad \text{(Porous medium shape factor)}. \tag{10}$$

The parameters F and s_{nf} are defined according to Hooman [21], and the system is subject to no-slip boundary conditions:

$$\widetilde{W} = 0 \ \text{ on } \ \partial\Omega. \tag{11}$$

Under the local thermal equilibrium assumption, the steady-state energy equation, neglecting heat generation, axial conduction, and thermal dispersion, is expressed in dimensional form as:

$$\rho_{nf} c_p w \frac{\partial T}{\partial z} = k \left(\frac{\partial^2 T}{\partial x^2} + \frac{\partial^2 T}{\partial y^2} \right). \tag{12}$$

The governing energy equation is non-dimensionalized using the variables from Eq. (2) and the definition of dimensionless temperature, $\theta = \frac{(T - T_w)}{(T_m - T_w)}$. This results in:

$$-Pe_{nf} \widetilde{W} \frac{\partial \theta}{\partial Z} = \frac{\partial^2 \theta}{\partial X^2} + \gamma^2 \frac{\partial^2 \theta}{\partial Y^2}, \tag{13}$$

where:

$$Pe_{\mathrm{nf}} = \frac{\rho_{\mathrm{nf}} c_p u_R a P^*}{\alpha_{\mathrm{nf}}} \qquad \text{(Nanofluid Péclet number)}, \tag{14}$$

$$T_m = \int_0^1 \int_0^1 T \, dY \, dX \qquad \text{(Mean temperature)}. \tag{15}$$

Heat transfer performance is characterized by the Nusselt number:

$$Nu = 2 \frac{q''}{k_{nf}(T_m - T_w)/h}. \tag{16}$$

The application of the first law of thermodynamics in dimensionless form yields:

$$\frac{\partial \theta}{\partial Z} = \frac{h q''}{k_{nf}(T_m - T_w)} \frac{1}{Pe}. \tag{17}$$

Combining Eqs. (16) and (17) gives:

$$Pe_{nf} \frac{\partial \theta}{\partial Z} = \frac{Nu}{2\widetilde{\alpha}}. \tag{18}$$

Where:

$$\widetilde{\alpha} = \frac{\alpha_{nf}}{\alpha_{bf}} \qquad \text{(Ratio of thermal diffusivities).} \quad (19)$$

The present formulation follows the scaling approach of Hooman [21], but employs a different normalization for the axial coordinate Z. In the fully developed regime, the temperature field exhibits distinct dependencies: the dimensionless temperature θ depends only on the transverse coordinates (X,Y), while the mean temperature T_m varies solely with Z. This behavior is embedded within the nondimensionalized first law of thermodynamics, where θ remains locally dependent on Z in its differential form, T_m evolves axially, and the velocity field $\widetilde{W}$ contributes via its spatial variation in the integral mean. Introducing the normalized temperature

$$\Theta = \frac{\theta}{Nu}, \quad (20)$$

we substitute Eqs. (18) and (20) into Eq. (13) to obtain the governing equation for the temperature field:

$$\frac{\partial^2\Theta}{\partial X^2} + \gamma^2\frac{\partial^2\Theta}{\partial Y^2} = -\frac{\widetilde{W}}{2\widetilde{\alpha}}. \quad (21)$$

The corresponding boundary conditions for Θ are specified as:

$$\begin{aligned} \left.\frac{\partial\Theta}{\partial X}\right|_{X=0} &= 0, \qquad \Theta|_{X=1} = 0, \\ \left.\frac{\partial\Theta}{\partial Y}\right|_{Y=0} &= 0, \qquad \Theta|_{Y=1} = 0, \end{aligned} \quad (22)$$

4 Numerical Scheme

The Brinkman-Forchheimer equation is nonlinear, so analytical solutions are impossible for multi-dimensional cases. Numerical methods must be adopted instead. In light of a two-dimensional domain that will be treated as rectangular for the purposes of the original solution developed here, the finite difference method on a uniform mesh is very well-suited. A central differencing scheme is adopted for high accuracy. For efficiency, the solution will utilise the alternate direction implicit (ADI) scheme. Although it is a two-dimensional problem, the ADI method decomposes it into manageable one-dimensional stages, resulting in enhanced convergence and stability. The FDM-ADI system effectively balances the accuracy in addressing complex heat transport problems within rectangular domains.

The numerical solution utilizes central differencing for spatial derivatives. The ADI scheme is implemented with implicit treatment in the x-direction and explicit treatment in the y-direction. Given the one-way coupling from the momentum to the energy equation, the flow field (Eq. 8) is solved first, independently of the temperature distribution. The Laplacian terms are discretized using a standard central difference approximation on a uniform grid with spacings ΔX and ΔY. The finite difference approximation for the

Brinkman-Forchheimer equation at the nodal point $\widetilde{W}_{i,j}$, where $X_i = i\Delta X$ and $Y_j = j\Delta Y$, is given by:

$$\frac{\widetilde{W}_{i-1,j} - 2\widetilde{W}_{i,j} + \widetilde{W}_{i+1,j}}{h^2} + \gamma^2 \frac{\widetilde{W}_{i,j-1} - 2\widetilde{W}_{i,j} + \widetilde{W}_{i,j+1}}{k^2} - s^2\widetilde{W}_{i,j} - Fs\widetilde{W}_{i,j}^2 = \Lambda. \quad (23)$$

Using a finite difference approximation [20] on equally spaced grid points, Eq. 8 is discretized, incorporating the Laplacian, Darcy, and Forchheimer terms into the following form:

$$(\widetilde{W}_{XX} + \gamma^2\widetilde{W}_{YY} - s^2\widetilde{W} + F\widetilde{W}^2) = \alpha_0\widetilde{W}(X_i, Y_j) + \alpha_1(\widetilde{W}X_{i+h_1}, j) + \alpha_2\widetilde{W}(X_{i,Y+h_2}) + \alpha_3\widetilde{W}(X_{i-h_3,j}) + \alpha_4\widetilde{W}(X_{i,j-h_4}). \quad (24)$$

A Taylor series expansion is used to derive the coefficients α_i, where h_1, h_2, h_3, and h_4 represent the step sizes in different spatial directions. This yields :

$$\begin{aligned} \alpha_0 &= s^2 - \frac{2}{h_1^2} - \frac{2\gamma}{h_2^2}, \\ \alpha_1 &= \frac{1}{h_1^2}, \quad \alpha_2 = \frac{\gamma}{h_2^2}, \\ \alpha_3 &= \frac{1}{h_3^2}, \quad \alpha_4 = \frac{\gamma}{h_4^2}. \end{aligned} \quad (25)$$

To facilitate an iterative solution procedure, the nonlinear Forchheimer term is quasi-linearized as follows:

$$\widetilde{W}^2 \approx \widetilde{W}_{i,j}^{(n)}\widetilde{W}_{i,j}^{(n+1)}, \quad (26)$$

where (n) and $(n+1)$ denote the current and subsequent iterations. The resulting linear system is solved via the ADI method, where each directional sweep is handled by Thomas' tridiagonal matrix algorithm.

5 Grid Independence Study

A grid independence study is conducted to ensure the accuracy of the numerical solutions for Brinkman-Forchheimer heat transfer in rectangular enclosures. Starting from a coarse mesh, the grid is systematically refined until key flow and thermal characteristics become invariant with further increases in resolution across all aspect ratios studied.

Grid independence was assessed using four systematically refined meshes: a coarse baseline ($\Delta X = 1/8$), an intermediate grid ($\Delta X = 1/16$), a fine grid ($\Delta X = 1/32$) and an ultra-fine grid ($\Delta X = 1/64$), corresponding to refinements $1\times$, $2\times$, $4\times$, and $8\times$, respectively. Initial computations on the coarse grid ($\Delta X = 1/8$) captured the global flow and thermal patterns but exhibited significant discretization errors, especially in boundary layers where Brinkman and Forchheimer effects are dominant. Successively finer grids ($\Delta X = 1/16$ to $1/64$) employed a linear interpolation scheme to better resolve near-wall gradients. This approach successfully minimized numerical artifacts and enhanced the capture of critical boundary layer phenomena in all aspect ratios. At each refinement

level, the complete numerical solution was recomputed. Particular attention was paid to the resolution of the coupled viscous-inertial terms in the momentum equation and the thermal diffusion in the energy equation. The nonlinear Forchheimer drag was carefully handled via quasi-linearization to ensure stability throughout the refinement process.

Grid independence was established by analyzing the convergence of velocity profiles, local Nusselt number distributions, and bulk flow parameters. The relative errors between successive grid levels were quantified to select a final resolution that optimally balances computational cost with numerical accuracy. This analysis confirmed that the chosen grid adequately resolves all essential physics.

The computed velocity field $\widetilde{W}_{i,j}$ was then used as input to solve the coupled boundary value problem of Eqs. (21)-(22) for the temperature distribution $\Theta(X,Y)$. This thermal solution employed a numerical procedure analogous to the velocity calculation, ensuring methodological consistency.

Finally, with $\widetilde{W}(X,Y)$ and $\Theta(X,Y)$ determined across the domain, the heat transfer performance was quantified via the Nusselt number Nu. The physical temperature field is given by $\theta(X,Y) = Nu\Theta(X,Y)$. Applying the normalization condition

$$\int_0^1 \int_0^1 \theta \widetilde{W} dX dY = 1 \tag{27}$$

to the discrete solutions yields an explicit expression for the Nusselt number:

$$Nu = \left(\int_0^1 \int_0^1 \Theta \widetilde{W} dX dY \right)^{-1}. \tag{28}$$

The integral in Eq. (28) is evaluated numerically using the two-dimensional trapezoidal rule. This method consistently accounts for the dependence of Nu on the parameters s and F, maintaining numerical consistency with the underlying finite difference scheme while ensuring efficient computation over the entire domain.

6 Analysis and Discussion

This paper investigates the Brinkman-Forchheimer flow in a rectangular cross-section porous medium saturated with a water-based molybdenum disulphide (MoS_2) nanoliquid. The thermophysical properties of the base fluid (water) and the nanoparticles (MoS_2) used in this numerical study are documented in Table 1. These values, measured at 300 K, are sourced from established experimental works (see, for example, *Sandeep et al.* [22] and *Siddheshwar and Veena* [23]).

The empirical correlations used to determine the effective thermophysical properties of the water-MoS_2 nanoliquid are summarised in Table 2, where ϕ represents the volume fraction of MoS_2 nanoparticles. The properties of the constituent materials required for these models are provided in Table 1.

The effective properties of the nanoliquid are computed using the base fluid properties from Table 1 and the correlation models from Table 2. Calculations are performed for nanoparticle volume fractions of $\phi = 0.03$ and 0.04, representing dilute concentrations that ensure well-dispersed nanoparticles. This ensures that agglomeration (or clustering) is minimized, as such phenomena would reduce the available surface area of the

nanoparticles for heat transfer, thereby defeating the purpose of enhancing the thermal conductivity of the base fluid.

Table 1: Thermophysical properties of water and MoS_2.

Quantity	**Water**	MoS_2
Density (kg/m^3)	997.1	5060
Thermal expansion coefficient ($K^{-1} \times 10^5$)	21	2.8424
Specific heat (J/kg·K)	4179	397.21
Thermal conductivity (W/m·K)	0.613	904.4
Dynamic viscosity (kg/m·s)	0.00089	–

This section presents a detailed analysis of the heat transfer performance within a porous medium saturated with a water-based molybdenum disulphide (MoS_2) nanofluid. The primary focus is to evaluate the impact of dilute concentrations of MoS_2 nanoparticles on the Nusselt number (Nu). The analysis investigates two specific nanoparticle volume fractions, $\phi = 0.03$ and $\phi = 0.04$, to quantify the effect of particle loading on heat transfer enhancement.

Nanofluids, which are stable suspensions of nanoparticles in a base fluid like water, are known to significantly improve thermal transport properties. In this study, the flow of the water-MoS_2 suspension through the porous structure is laminar and fully developed. The analysis examines the interplay between the nanoparticle volume fraction (ϕ) and the Forchheimer number (F), which characterizes the inertial flow resistance within the porous medium.

By systematically varying the nanoparticle concentration, this study aims to identify the optimal dilution of MoS_2 for maximizing the Nusselt number, a direct indicator of convective heat transfer efficiency. The results provide valuable insights into the role of dilute nanoparticle suspensions in enhancing thermal performance, with potential applications in advanced cooling systems and compact heat exchangers.

6.1 Thermal Characteristics of the Water-MoS_2 Mixture

The dispersion of Molybdenum Disulphide (MoS_2) nanoparticles in water significantly enhances the thermal conductivity of the base fluid, leading to improved heat transfer performance within porous enclosures. This enhancement is strongly influenced by the geometric complexity of the porous matrix and the concentration of nanoparticles.

Table 3 displays the Nusselt number (Nu) for the water-MoS_2 mixture across a range of shape factors (s) at two Forchheimer numbers, $F = 1$ and $F = 2$, and for two nanoparticle volume fractions, $\phi = 0.03$ and $\phi = 0.04$. A consistent increase in Nu is observed with increasing s, indicating that more complex pore geometries enhance convective heat transfer. Furthermore, a higher nanoparticle concentration consistently yields a higher Nu, underscoring the role of improved thermal conductivity in nanofluids. The percentage increases shown are calculated relative to the baseline Nusselt number at $s = 10^{-2}$ for the respective F and ϕ values, demonstrating the total enhancement achieved across the range of the shape factor.

Table 2: Models to determine the thermophysical properties of the nanoliquids.

Model	Thermophysical Property
Hamilton–Crosser model	$\frac{k_{nl}}{k_{bl}} = \frac{\left(\frac{k_{np}}{k_{bl}}+2\right) - 2\phi\left(1-\frac{k_{np}}{k_{bl}}\right)}{\left(\frac{k_{np}}{k_{bl}}+2\right) + \phi\left(1-\frac{k_{np}}{k_{bl}}\right)}$ (Hamilton & Crosser, 1962)
Brinkman model	$\frac{\mu_{nl}}{\mu_{bl}} = \frac{1}{(1-\phi)^{2.5}}, \quad (\phi < 0.06)$ (Brinkman, 1952)
Mixture theory	$\frac{(\rho c_p)_{nl}}{(\rho c_p)_{bl}} = (1-\chi) + \chi\frac{(\rho c_p)_{np}}{(\rho c_p)_{bl}}$ $\frac{(\rho\beta)_{nl}}{(\rho\beta)_{bl}} = (1-\phi) + \phi\frac{(\rho\beta)_{np}}{(\rho\beta)_{bl}}$ $\frac{\rho_{nl}}{\rho_{bl}} = (1-\phi) + \phi\frac{\rho_{np}}{\rho_{bl}}$
Other relations	$c_{p_{nl}} = \frac{(\rho c_p)_{nl}}{\rho_{nl}}, \quad \beta_{nl} = \frac{(\rho\beta)_{nl}}{\rho_{nl}}, \quad \alpha_{nl} = \frac{k_{nl}}{(\rho c_p)_{nl}}$

For instance, at $F = 1$ and $\phi = 0.03$, Nu increases from 4.370 at $s = 10^{-2}$ to 6.3247 at $s = 10^2$, representing a significant cumulative enhancement of 44.69%. For the higher concentration of $\phi = 0.04$, the values rise from 5.5730 to 7.4914, marking a 34.37% increase. A similar trend is evident at $F = 2$, where the Nusselt number at $s = 10^2$ shows a 28.64% and 24.02% total increase for $\phi = 0.03$ and $\phi = 0.04$, respectively, from their baseline values.

The relationship between the shape factor and heat transfer enhancement is further illustrated in Figure 2, which plots Nu against $\log(s)$. The curves for both volume fractions and Forchheimer numbers show a steady upward trend, confirming the positive influence of both the nanoparticle concentration and the geometric complexity. The cumulative percentage increases reveal a substantial overall improvement in thermal performance, highlighting the effectiveness of the water-MoS_2 nanofluid in enhancing heat transfer within porous media.

7 Conclusion

This study presents a comprehensive numerical analysis of forced convection heat transfer for a water-Molybdenum Disulphide (MoS_2) nanofluid within a three-dimensional porous rectangular enclosure, based on the Darcy-Brinkman-Forchheimer model. The governing equations were solved using a robust finite difference method (FDM) combined with the Alternating Direction Implicit (ADI) scheme, ensuring computational efficiency and stability. A systematic grid independence study was conducted to guarantee the accuracy of the results. The investigation yielded the following principal conclusions:

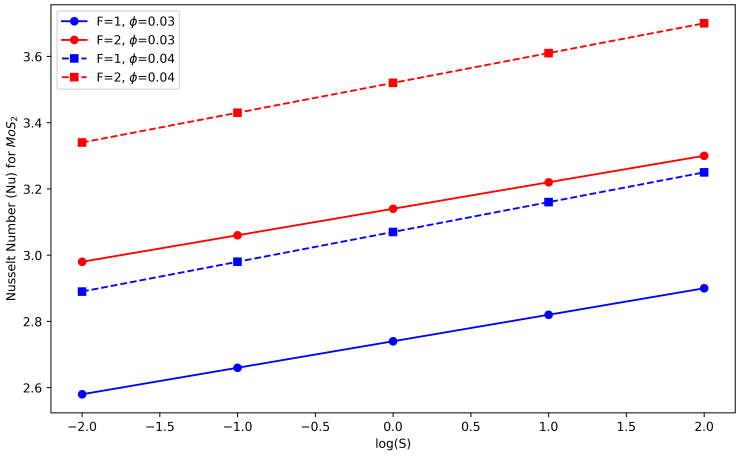

Figure 2: Effect of F and ϕ on Nu for water - MoS_2 mixture

Table 3: Table showing Nu values of water–MoS_2 mixture for different s values at $F = 1$ and $F = 2$.

$F = 1$					$F = 2$				
s	$Nu_{(\phi=0.03)}$	% increase	$Nu_{(\phi=0.04)}$	% increase	s	$Nu_{(\phi=0.03)}$	% increase	$Nu_{(\phi=0.04)}$	% increase
10^{-2}	4.370	–	5.5730	–	10^{-2}	6.8133	–	7.9710	–
10^{-1}	4.8587	11.81%	6.0530	8.62%	10^{-1}	7.3020	7.18%	8.4506	6.02%
10^{0}	5.3473	22.38%	6.5322	17.20%	10^{0}	7.7907	14.34%	8.9300	12.03%
10^{1}	5.8360	33.58%	7.0118	25.83%	10^{1}	8.2793	21.51%	9.4098	18.05%
10^{2}	6.3247	44.69%	7.4914	34.37%	10^{2}	8.7680	28.64%	9.8890	24.02%

1. The addition of MoS_2 nanoparticles to the base fluid (water) significantly enhances the thermal performance of the system. This is evidenced by a consistent and substantial increase in the Nusselt number (Nu) with an increase in the nanoparticle volume fraction (ϕ), across all values of the shape factor (s) and Forchheimer number (F).

2. The shape factor (s) of the porous medium plays a critical role in heat transfer augmentation. The results demonstrate a strong positive correlation between s and the Nusselt number, indicating that more complex pore geometries significantly intensify convective heat transfer. The percentage increase in Nu was calculated cumulatively from a baseline, revealing enhancements of up to 44.69% for $F = 1$ and $\phi = 0.03$ over the investigated range of s.

3. The Forchheimer number (F), representing the inertial resistance within the porous medium, also has a pronounced effect. Higher F values consistently resulted in higher Nusselt numbers for identical combinations of ϕ and s, highlighting the

importance of accounting for inertial effects in high-velocity flow regimes within porous media.

4. The numerical methodology, employing central differencing and quasi - linearization of the nonlinear Forchheimer term, proved to be highly effective and stable. The FDM-ADI framework provided an optimal balance between computational cost and solution accuracy for the rectangular domain under consideration.

The synergistic combination of a water-MoS_2 nanofluid and a porous medium with a high shape factor provides a highly effective means of enhancing heat transfer. The findings of this work offer valuable insights for the design and optimization of thermal systems, such as compact heat exchangers and advanced cooling devices, where managing high heat fluxes is critical.

References

[1] Masuda H., Ebata A., and Teramae K., "Alteration of thermal conductivity and viscosity of liquid by dispersing ultra-fine particles. dispersion of al2o3, sio2 and tio2 ultra-fine particles", 1993.

[2] Eastman J. A., Choi S. U. S., Li S., Yu W, and Thompson L., "Anomalously increased effective thermal conductivities of ethylene glycol-based nanofluids containing copper nanoparticles", *Applied physics letters*, vol. 78, (6), pp. 718–720, 2001.

[3] Das S. K., Putra N. S. D., Thiesen P., and Roetzel W., "Temperature dependence of thermal conductivity enhancement for nanofluids", *Journal of heat transfer*, vol. 125, (4), pp. 567–574, 2003.

[4] Choi S. U. S., "Enhancing thermal conductivity of fluids with nanoparticles", in *ASME international mechanical engineering congress and exposition*, American Society of Mechanical Engineers, vol. 17421, 1995, pp. 99–105.

[5] Minkowycz W., Sparrow E. M., and Abraham J. P., *Nanoparticle heat transfer and fluid flow*. CRC press, 2012, vol. 4.

[6] Khanafer K., Vafai K., and Lightstone M., "Buoyancy-driven heat transfer enhancement in a two-dimensional enclosure utilizing nanofluids", *International journal of heat and mass transfer*, vol. 46, (19), pp. 3639–3653, 2003.

[7] Siddheshwar P. G. and Meenakshi N, "Amplitude equation and heat transport for Rayleigh–Bénard convection in newtonian liquids with nanoparticles", *International Journal of Applied and Computational Mathematics*, vol. 3, (1), pp. 271–292, 2017.

[8] Buongiorno J., "Convective transport in nanofluids", 2006.

[9] Siddheshwar P. G., Kanchana C, Kakimoto Y, and Nakayama A., "Steady finite-amplitude Rayleigh–Bénard convection in nanoliquids using a two-phase model: Theoretical answer to the phenomenon of enhanced heat transfer", *Journal of Heat Transfer*, vol. 139, (1), p. 012 402, 2017.

[10] Kanchana C and Laroze D., "Study of chaos in Rayleigh-Benard convection of water-alumina nanofluid with heat source sink", *CU Journal of Non-Linear Fluid Mechanics*, vol. 1, (01), pp. 1–15, 2025.

[11] Darcy H., *Les fontaines publiques de la ville de Dijon: Exposition et application des principes à suivre et des formules à employer dans les questions de distribution d'eau: Ouvrage terminé par un appendice relatif aux fournitures d'eau de plusieurs villes, au filtrage des eaux et à la fabrication des tuyaux de fonte, de plomb, de tôle et de bitume*. Victor Dalmont, éditeur, 1856, vol. 2.

[12] Brinkman H. C., "A calculation of the viscous force exerted by a flowing fluid on a dense swarm of particles", *Flow, Turbulence and Combustion*, vol. 1, (1), pp. 27–34, 1949.

[13] Forchheimer P., "Wasserbewegung", *Ver. Dtsch. Ing.*, vol. 45, pp. 1782–1788, 1901.

[14] Vafai K. and Tien C. L., "Boundary and inertia effects on flow and heat transfer in porous media", *International Journal of Heat and Mass Transfer*, vol. 24, (2), pp. 195–203, 1981.

[15] Rudraiah N, Siddheshwar P. G., Pal D, and Vortmeyer D, "Non-darcy effects on transient dispersion in porous media", in *ASME Proc. Nat. Heat Trans. Conf., Houston, Texas USA*, vol. 96, 1988, pp. 623–635.

[16] Bear J. and Bachmat Y., *Introduction to modeling of transport phenomena in porous media*. Springer Science & Business Media, 2012, vol. 4.

[17] Patankar S., *Numerical heat transfer and fluid flow*. CRC press, 2018.

[18] Bellman R. E. and Kalaba R. E., "Quasilinearization and nonlinear boundary-value problems", *(No Title)*, 1965.

[19] Sam N. E., Nagouda S. S., and Siddheshwar P. G., "Darcy–Forchheimer–Brinkman flow of a newtonian fluid through an enclosure with two straight boundaries and one curved boundary", *International Journal of Applied and Computational Mathematics*, vol. 11, (5), p. 195, 2025.

[20] Jain M. K., Iyengar S. R. K., and Jain R. K., *Numerical methods: problems and solutions*. New Age International, 2007.

[21] Hooman K., "A perturbation solution for forced convection in a porous-saturated duct", *Journal of computational and applied mathematics*, vol. 211, (1), pp. 57–66, 2008.

[22] Sandeep N, Sharma R. P., and Ferdows M., "Enhanced heat transfer in unsteady magnetohydrodynamic nanofluid flow embedded with aluminum alloy nanoparticles", *Journal of Molecular Liquids*, vol. 234, pp. 437–443, 2017.

[23] Siddheshwar P. G. and Veena B. N., "Study of Brinkman–Bénard nanofluid convection with idealistic and realistic boundary conditions and by considering the effects of shape of nanoparticles", *Heat Transfer*, vol. 50, (4), pp. 3948–3976, 2021.

Acknowledgements

The authors would like to thank the Department of Mathematics, Christ University, for providing the necessary computational facilities and support.

Data Availability

The data that support the findings of this study are available from the corresponding author upon request.